Thermodynamic study of monolayer methane on graphite

H. K. Kim,* Q. M. Zhang, and M. H. W. Chan
Department of Physics, The Pennsylvania State University, University Park, Pennsylvania 16802
(Received 6 May 1986)

High-resolution heat-capacity and vapor-pressure isotherm measurements have been made to study the phases and phase transitions of monolayer methane on graphite. In the submonolayer region, heat-capacity results indicate a continuous transition between the $\sqrt{3}\times\sqrt{3}$ commensurate solid (CS) phase and an expanded incommensurate solid (ES) phase and triple-point melting from the ES phase. Within the resolution of our data no heat-capacity evidence of an orientational ordering transition is found. The liquid-vapor coexistence boundary is studied very carefully and the results show that the critical point of methane on graphite belongs to the two-dimensional Ising universality class. In the pure-solid-phase near-monolayer-completion region, the transition from the compressed or dense incommensurate solid (DS) phase to the ES phase and melting from the ES phase are studied. Both heat-capacity and vapor-pressure isotherm data show evidence of the existence of a thin sliver of $(\sqrt{3}\times\sqrt{3})$ phase sandwiched between the DS and ES phases. This thin sliver of CS phase terminates near a coverage of $n_e=1$ and $T=88$ K. Beyond this coverage and temperature, the transition between the DS and ES phases becomes continuous. The melting transition from the ES phase is found to be first order in all the coverages studied in this experiment. The isotopic effect is studied for the commensurate-incommensurate, melting, and liquid-vapor critical transitions.

I. INTRODUCTION

Among the large number of physisorption systems, monolayer methane on graphite is one of the most frequently studied. This is the case because in this overlayer system there are many interesting two-dimensional phase transitions. Two-dimensional melting, liquid-vapor orientational ordering, and commensurate-incommensurate transitions all take place at convenient temperatures.

Experimental studies of methane on graphite include neutron scattering (Refs. 1–3), NMR (Refs. 4 and 5) and calorimetric (Refs. 6 and 7), quasielastic neutron scattering (Ref. 8), vapor pressure (Ref. 9), heat of adsorption (Ref. 10), and low-energy electron diffraction (Ref. 11) methods. Neutron studies provide a two-dimensional phase diagram with $(\sqrt{3}\times\sqrt{3})$ commensurate (CS), expanded (ES), and compressed or dense (DS) solid phases and a disordered fluid phase.[1] The commensurate-incommensurate transition (CIT) between the CS and DS phases as well as that between the CS and ES phases were found to be continuous. In the submonolayer region, at low temperatures, the absorbed layer is in the $(\sqrt{3}\times\sqrt{3})$ CS phase and a CIT to the ES phase is found near 50 K. The CIT temperature shifts up to 68 K as coverage is increased in the pure solid phase. In the neutron study, the DS phase is found in a coverage range above that of the CS phase. In the high-temperature and the high-surface-coverage region, the neutron results suggest that the DS phase smoothly changes into the ES phase without locking into a commensurate region.[1] Melting of methane on graphite was found to occur always from the ES phase. The melting transition takes place at a triple point near 60 K in the submonolayer region and the transition temperature shifts upwards with increasing surface coverage in the near-monolayer-completion region and the transition is first order. The quasielastic neutron technique[8] has also been used to measure the diffusion coefficient of CH_4 adsorbed on graphite in the submonolayer region. In this study, a coexistence region of liquid and vapor below and a region of uniform hypercritical fluid above the two-dimensional critical temperature were found. This finding is consistent with an earlier vapor-pressure isotherm experiment.[9]

The NMR study of Quateman and Bretz[4] confirmed to a large extent the results of the neutron scattering studies.[1–3] In this NMR experiment, as in the neutron scattering studies, no evidence of an order-disorder transition of the orientation of methane molecular axes in the submonolayer region was found. Such a transition was reported in a more recent NMR study.[5]

The CIT from the CS to the ES phases and the melting transition have been studied in a heat-capacity experiment by Marx *et al.*[6] They found two heat-capacity peaks, a very broad weak anomaly at 47.6 K for the CIT and a prominent peak at 56.2 K for the melting transition. More recently, a heat-capacity experiment was performed to study the liquid-vapor transition.[7] They found a broad heat-capacity signal near 70 K corresponding to a liquid-vapor transition in addition to the sharp melting peak at 56.5 K. The location of the critical temperature and the shape of the liquid-vapor coexistence boundary are in agreement with the results to be presented below.

In this paper, we will present the results of a comprehensive thermodynamic study of CH_4 on graphite in both the submonolayer and near-monolayer regions. In our study, heat-capacity scans at constant coverages were complemented by isotherm measurements in locating the boundaries between different two-dimensional phases and

determining the nature of the phase transition between these phases. In our study, a total of 46 heat-capacity scans of different surface coverages ranging between $n=0.07$ and 1.30 were made from $T=4$ to 105 K. Vapor-pressure isotherms were made at six different temperatures between $T=70$ and 100 K.

In order to study the isotopic effect on the various two-dimensional phase transitions, heat-capacity measurements of nine different surface coverages of CD_4 on graphite in addition to the CH_4 scans were made. Some of the results related to the two-dimensional liquid-vapor transition, particularly the shape of the boundary of this coexistence region, have already been published.[12] In this paper our discussion regarding the liquid-vapor transition will complement the earlier paper. In a companion study, the multilayer growth mode of CD_4 and CH_4 on graphite were studied from 4 to 40 K.[13] By following the evolution of the heat-capacity signal related to the orientational ordering transition, we were able to conclude that methane grows layer by layer on graphite above 20 K and that near 11 K there is a structural change, possibly a wetting transition in the multilayer methane film.

The organization of this paper is as follows. In Sec. II, we will briefly describe the experimental setup and procedures; the phase diagram determined in this study is also presented. The results on the orientational ordering transition, commensurate-incommensurate transition, and melting transition in the submonolayer region will be presented in Secs. III, IV, and V, respectively. In Sec. VI some additional discussion of the liquid-vapor transition is presented. The melting and structural transition in the near-monolayer-completion region is presented in Sec. VII.

II. EXPERIMENTAL PROCEDURE AND PHASE DIAGRAM OF METHANE ON GRAPHITE

Two complementary thermodynamic methods were used in this study, namely a constant-surface-coverage heat-capacity scans as a function of temperature and vapor-pressure isotherm measurements. Heat-capacity scans are particularly sensitive to boundaries perpendicular to the temperature axis in a coverage-versus-temperature phase diagram and the vapor pressure isotherms are sensitive to those parallel to the temperature axis. Graphite Foam, a form of exfoliated graphite manufactured by Union Carbide, is used as the substrate in these studies. Graphite Foam with a surface area of 20 m^2/g, was found in a synchrotron x-ray study to have a single-crystal domain size of about $(1000\ \text{Å})^2$.[14] Following the convention of other methane studies, we define the coverage of $n=1$ at the inflection point between the first and second vertical steps of the vapor-pressure isotherm performed at 78 K. In this definition, $n=0.87$ corresponds to a coverage for the completion of a $(\sqrt{3}\times\sqrt{3})$ commensurate overlayer. These measurements were made in evaporation cryostats. For heat-capacity scans below 50 K, liquid helium was used as the cryogen. These scans were made to search for the orientational ordering transition of the two-dimensional (2D) film. For scans above 50 K, liquid nitrogen was used as the cryogen. For the adsorption isotherm experiment, pressure was measured with an *in situ* diaphragm capacitance gauge. This gauge was calibrated against a commercial gauge at room temperature. The *in situ* gauge eliminates problems due to thermomolecular correction at low pressures, slow response time between a room-temperature gauge and the graphite sample through the thin filling capillary, and drifts in the pressure gauge related to temperature variations in the laboratory. The resolution in pressure determination of this gauge is one part per 20 000.[15]

The ac calorimetric technique used in this experiment has been described previously[16] and will not be repeated here. Due to the rapidly decreasing thermal conductivity of the Graphite Foam substrate, it is difficult to determine the absolute value of the heat capacity below 20 K. This is the case because with low thermal conductivity, the internal equilibrium time of the calorimeter is comparable to the inverse of the operating frequency. For $20\ \text{K} > T > 4$ K, the heat capacity of the calorimeter, which consists of a piece of Graphite Foam sandwiched between two sapphire disks, is calculated from the known specific heat of graphite and sapphire.[17] By comparing this calculated value to our measured value, a scaling factor is determined. The scaling factor is used to determine the heat-capacity contribution due to the adsorbed film. The calculated heat capacity values of the calorimeter for $T \geq 20$ K are in agreement with the measured values to within 8%. We estimate the accuracy of the total heat capacity of the methane film on graphite plus the calorimeter at temperature lower than 20 K to be 15%. However, there is no possibility in our normalization procedure to miss a heat-capacity anomaly of the adsorbed film in the low-temperature region. Our technique is capable of detecting heat-capacity anomalies with peak height of $0.3k_B$ per adsorbed molecule.

The proposed coverage-temperature phase diagram of submonolayer CH_4 on graphite due to this study is shown in Fig. 1. We relied on the results of the neutron studies to identify the structure of the various solid phases. In the high-temperature and high-coverage region of the phase diagram, the heat-capacity scan is not that of constant coverage. The experimental path followed in the scan curves towards lower coverage as a function of temperature due to desorption of adsorbate molecules into the sample cell volume.

The phase diagram of monolyer CH_4 on graphite given by our thermodynamic measurements is generally in agreement with that given by neutron scattering (Ref. 1) and NMR (Ref. 4) studies. In the region of high temperature and high coverage, our study indicates a thin sliver of commensurate solid (CS) between the incommensurate expanded (ES) and incommensurate dense (DS) solid. The neutron result did not find evidence of locking into the CS phase. Instead, a gradual and smooth change of the lattice constant from a DS value to one corresponding to the ES phase was found as temperature is increased through 90 K. The liquid-vapor coexistence boundary of our phase diagram is determined much more precisely than previous studies. Our result indicates that the liquid-vapor transition of methane on graphite belongs to the two-dimensional Ising universality class.

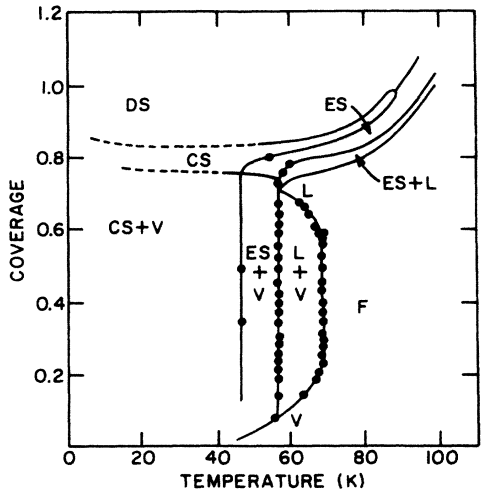

FIG. 1. Phase diagram of monolayer methane on graphite. Solid circles are locations of observed heat-capacity anomalies, and solid lines are phase boundaries. Dashed lines are more speculative phase boundaries. DS, CS, and ES stand for compressed (dense), commensurate, and expanded solid, respectively. L, V, and F stand for liquid, vapor, and hypercritical fluid, respectively. For the sake of clarity, locations of anomalies above $n=0.88$ are omitted. See Fig. 9 for an expanded plot in the high-coverage, higher-temperature region.

III. THE ORIENTATIONAL ORDERING TRANSITION

The orientational ordering of the axes of (nonspherical) adsorbate molecules has been observed in submonolayer N_2 (Ref. 18), CO (Ref. 19), and H_2 (Ref. 20) on graphite. It is found that with decreasing temperature, the commensurate $(\sqrt{3}\times\sqrt{3})$ solid phase of these linear molecules undergoes a transition from a disordered phase where the molecular axes are randomly oriented to an ordered phase where the molecular axes are oriented with respect to each other. The quadrupole-quadrupole interaction between these molecules is thought to be responsible for the ordering at low temperature.[21]

For methane, the octupole-octupole interaction, instead of the quadrupole-quadrupole interaction is responsible for the orientational ordering in bulk solids. Simulation studies using Monte Carlo and molecular field methods have been used to study the orientationally ordered phases in monolayer commensurate solid methane on graphite.[22] For a free-standing layer with no substrate field, it is predicted that the system displays three phases: a high-temperature disordered phase, an intermediate-temperature phase consisting of a random arrangement of stable and unstable tripods, and a low-temperature phase having alternating rows of stable and unstable tripods. According to a mean-field calculation including the effect of the crystal field of graphite, the methane molecules are found to sit as stable tripods; at high temperature, the methane molecules are in free rotation about the tripod axis, and at low temperature, the motion is strongly hindered and the methane are orientationally ordered.[23]

Inelastic neutron scattering experiments by Newberry *et al.* and Smalley *et al.* have shown evidences that at low temperatures, the CH_4 commensurate monolayer is orientationally ordered.[24] Two sharp side peaks on the incoherent neutron scattering spectrum were observed for monolayer methane on graphite below 30 K. The tunneling spectrum gradually becomes diffuse as the temperature is raised, and disappears for $T>30$ K. A possible explanation of this result is that methane molecules on graphite are orientationally ordered at low temperature and gradually becoming more disordered with increasing temperature. It is not clear whether this is a signature of an orientational phase transition in the methane monolayer. A recent NMR study[5] found a minimum in the spin-lattice relaxation time near 17 K. They interpreted this minimum to be due to the orientational ordering transition from the isotropic orientation phase to the orientationally ordered phase. Neutron diffraction measurements of submonolayer CD_4 (Ref. 1) showed no evidence of orientational ordering transition down to 6 K.

In order to search for the orientational ordering transition in the submonolayer coverage, heat-capacity measurements were carried out for five different surface coverages of CH_4 and four different surface coverages of CD_4 ranging from $n=0.3$ to 1.0.

Figure 2 shows heat-capacity scans of five different CH_4 and CD_4 coverages in the temperature interval of $5\text{ K}<T<40$ K. In these scans, as in other scans shown in subsequent figures, the heat-capacity contribution due to the calorimeter has been subtracted. We did not find any sign of phase transition in this temperature region for

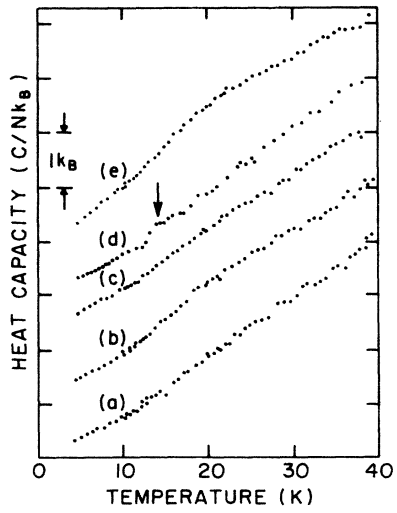

FIG. 2. Heat-capacity scans of submonolayer CH_4 (bottom two scans) and CD_4 (top three scans) on graphite at low temperature (5—40 K). Heat capacities are shown in C/Nk_B units, where N is the total number of methane molecules on graphite. Heat-capacity contribution due to the calorimeter is subtracted. Scans are shown for coverages (a) 0.50 CH_4, (b) 0.85 CH_4, (c) 0.81 CD_4, (d) 0.85 CD_4, and (e) 1.00 CD_4.

submonolayer CH_4. For CD_4, only one of the four coverages studied, at $n=0.85$, shows a small bump (height $\sim 0.3k_B$) near 13 K. This bump is located by an arrow in Fig. 2. It is possible that this peak at $n=0.85$ is related to the crossing of the boundary separating the DS and CS phases. In our coverages scale, $n=0.87$ is the ideal $(\sqrt{3}\times\sqrt{3})$ completion coverage and the DS-CS boundary may not be entirely parallel to the temperature axis at low temperatures. The smoothly increasing heat capacity as a function of temperature for all coverages is due to the Debye contribution of a two-dimensional solid. The concave regular heat-capacity contribution at temperatures lower than 10 K is expected from the quadratic temperature dependence of the heat capacity of a two-dimensional-like solid at low temperatures.[25]

It is not completely clear why our heat capacity and the neutron diffraction studies failed to find evidence of an orientational ordering transition in contrast to the NMR (Ref. 5) and inelastic neutron (Ref. 24) results. It is possible that the heat of transition is exceedingly small and the transition is gradual. Another possibility is that the axes of the methane molecules are gradually frozen into an orientationally ordered structure with decreasing temperature without going through a cooperative transition. It should be pointed out that in our study of multilayer CH_4 and CD_4 on graphite,[13] heat-capacity peaks related to orientational ordering transition were observed for $n \geq 2$.

IV. THE COMMENSURATE-INCOMMENSURATE TRANSITION

Figure 3 shows six traces of heat capacity as a function of temperature in the vicinity of the transition between CS and ES for both CH_4 and CD_4.[1] The peak height is on the order of $1k_B$ per molecule and the full width at half maximum (FWHM) of these peaks is on the order of 2 K. The peak position is found to be coverage independent in the submonolayer coverage region ($n<0.75$). These features are summarized in Table I. In the submonolayer region a 2D vapor coexists with the solid phases. The peak position for CH_4 (47 K) is slightly lower than that for CD_4 (48.5 K). Such an isotopic effect is shown not only in CIT but also in liquid-vapor and melting transitions. The isotopic effect on the transition temperature in CIT is opposite of that observed in melting and liquid-vapor transitions. A discussion of the isotopic effect on the various two-dimensional transitions of methane on graphite will be presented in the section of liquid-vapor transition.

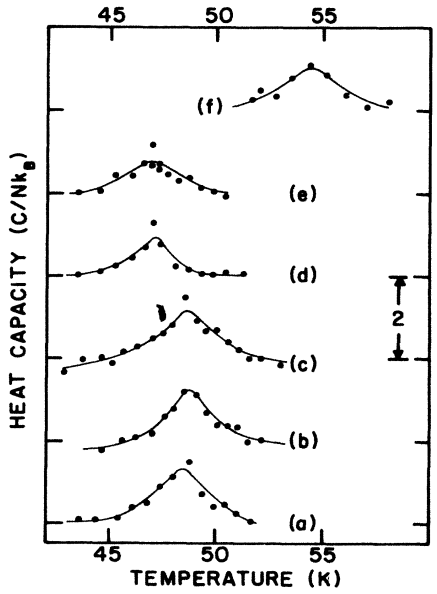

FIG. 3. Heat-capacity scans of commensurate-incommensurate transition of submonolayer methane (bottom three scans for CH_4 and top three scans for CD_4) on graphite. The surface coverages are (a) 0.330 CD_4, (b) 0.500 CD_4, (c) 0.667 CD_4, (d) 0.351 CH_4, (e) 0.503 CH_4, and (f) 0.805 CH_4.

TABLE I. Commensurate-incommensurate (ES) transition of submonolayer methane on graphite. T_p, FWHM, and height represent temperature, full width at half maximum, and height of the heat-capacity peak, respectively. ΔH represents heat of transition. Height and ΔH are given in reduced units of k_B per adsorbed molecule and k_BK per adsorbed molecule, respectively. The coverage and temperature scales are accurate to $\Delta n \simeq 0.01$ and 0.2 K. The (relative) uncertainty in n and T are, respectively, 0.005 and 0.01 K.

	Coverage (n)	T_p (K)	FWHM (K)	Height (k_B)	ΔH (k_BK)
CH_4	0.351	47.0	1.8	1.2	3.0
	0.503	47.0	2.0	1.0	2.7
	0.805	54.5	2.5	1.1	3.5
CD_4	0.330	48.5	2.0	1.2	3.0
	0.500	48.8	2.2	1.2	3.5
	0.667	48.8	2.5	1.1	3.8

The physical mechanism of this type of CIT appears to be related to the fact that above the transition temperature, the thermal energy available to the overlayer is sufficient to drive the methane molecules away from the commensurate sites and the stable phase is an incommensurate ES phase. An anharmonic finite-temperature calculation[26] based on this picture found a transition at 44 K, in reasonable agreement with our result. The prediction of first-order transition of this calculation does not appear to be consistent with the observed broad heat capacity anomalies shown in Fig. 3. Previous heat-capacity[5] and neutron diffraction[1-3] results also suggest this transition to be continuous. Figure 1 also shows CIT between pure CS, DS, and ES phases at near monolayer completion coverage. The nature of these transitions seems to be different from that between the CS and ES phases with coexisting 2D vapor. These transitions will be discussed in a later section.

V. MELTING TRANSITIONS IN SUBMONOLAYER REGION

In Fig. 4, six out of the eighteen heat-capacity traces of submonolayer methane (CH_4 and CD_4) films near 57 K are shown. The heat-capacity values in these traces are

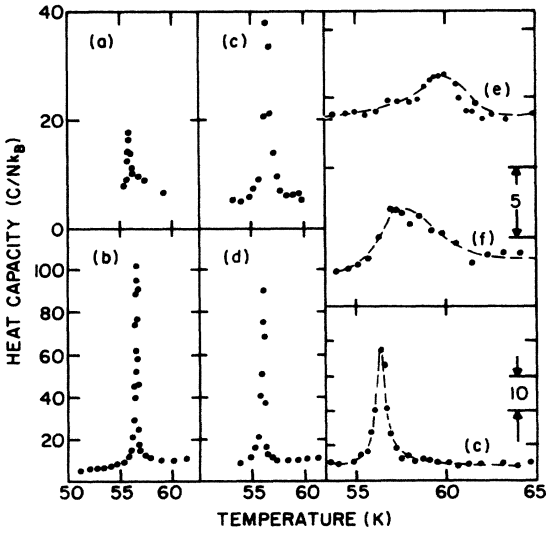

FIG. 4. Heat-capacity scans of melting transition of submonolayer methane on graphite. The coverages are (a) 0.076 CH_4, (b) 0.525 CH_4, (c) 0.704 CH_4, (d) 0.381 CD_4, (e) 0.751 CH_4, and (f) 0.775 CH_4.

also expressed in reduced units of k_B per molecule. The δ-function-like heat-capacity peak with a full width at half maximum of 0.15 K is found at the same temperature of 56.58 K for scans with coverages between $n=0.145$ and 0.62. The constancy of the peak temperature and the narrow width of these peaks in this coverage range are consistent with triple-point interpretation at this temperature. In addition to methane on graphite, triple-point melting has been observed in a number of other systems: Xe on graphite,[27] Ne on graphite,[28] and O_2 on graphite[29] which melt from incommensurate solid phases and CF_4 on graphite, which melts from a (2×2) commensurate overlayer.[30] Our results are in good agreement with an earlier heat-capacity study[6] except that a sharper peak is found in our study. The δ-function-like heat-capacity peaks confirm the conclusion of the NMR and neutron diffraction studies that the melting transition is first-order in the submonolayer region.

We found the reduced height of the heat-capacity peak grows with coverage for $n \lesssim 0.2$, and decreases with coverage for $n \gtrsim 0.63$. The peak height remains constant at a reduced value of $C/Nk_B=90\pm10$ between $n=0.2$ and 0.55. For $n \lesssim 0.2$, according to the lever rule, the proportion of the molecules in the two-dimensional vapor phase is substantial and this reduces the percentage of molecules that are involved in the melting transition. The heat-capacity anomaly for the $n=0.08$ scan appears at a temperature 0.5 K lower than the triple-point temperature. It is likely that this heat-capacity peak is a signature of sublimation rather than melting. Above $n=0.67$, the FWHM of the heat-capacity peak increases substantially indicating that melting is no longer taking place at a triple point but through a solid-liquid coexistence region. In addition to a shift to higher melting temperature, the heat-capacity peak for the scans between $n=0.7$ and 0.77 is significantly broadened. The increase in half width reflects the crossing of the solid-liquid coexistence region as well as the fact that the melting boundary is becoming less perpendicular to the temperature axis. Near $n=0.80$ the shift towards higher melting temperature with coverage is particularly significant. The melting characteristics for coverages beyond $n=0.80$ will be discussed in a later section.

Figure 4 also shows a trace for the melting transition of CD_4. The triple-point temperature of CD_4 on graphite is nearly 0.5 K lower than that of CH_4 on graphite. This isotopic effect appears in the inverse direction to that of commensurate-incommensurate transition. A similar isotopic effect is observed in the bulk melting transition. The triple point for CD_4 is 89.78 K and that of CH_4 is 90.64 K.[31] It is also seen in another two-dimensional system, namely ethylene on graphite. The melting temperature for submonolayer C_2D_4 is 67.8 K and that of C_2H_4 is 68.2 K.[32] As stated earlier, a discussion of the isotopic effect will be presented in the section on liquid-vapor transition. The characteristics of the melting peak for methane on graphite from submonolayer to near monolayer completion coverage are shown in Table II.

VI. THE LIQUID-VAPOR TRANSITION

The results of the liquid-vapor transition of methane on graphite, particularly the shape of the coexistence boundary have been published.[12] The coexistence boundary is determined by locating the peak temperature of the heat-capacity anomaly related to the crossing of the liquid-vapor coexistence boundary as a function of surface coverage. The heat-capacity anomaly at a number of surface coverages is shown in Fig. 5. Since the location of this boundary, $n(T)$ also denotes either the two-dimensional liquid (if $n > n_c$) or vapor (if $n < n_c$) areal density, the observed boundary can be used to fit the power law

$$(n_l - n_c) = (n_c - n_v) = B(T_c - T)^{\beta},$$

where n_c, n_l and n_v are, respectively, the critical, liquid, and vapor areal densities and T_c the critical temperature. Out data yield a critical exponent β of 0.127 ± 0.02. This is in very good agreement with $\frac{1}{8}$, the value expected from the two-dimensional Ising model.[33] This result shows that the liquid-vapor critical point of methane on graphite does belong to the two-dimensional Ising universality class.

The critical temperature of CH_4 on graphite is determined in our experiment to be at 68.77 ± 0.06 K. This is considerably lower than the 75 K inferred from the vapor pressure isotherm and heat of adsorption studies.[9,10] As stated above, the location of the critical temperature according to another heat-capacity study, is consistent with our result.[7] Similar difference between heat-capacity and vapor pressure isotherm studies are found in a number of other systems. For Ar on graphite, the critical temperature according to a heat-capacity study is 53 K (Ref. 34) and that due to a vapor pressure isotherm study is 58 K (Ref. 35). For CF_4 on graphite, the respective values are 93 (Ref. 30) and 99 K (Ref. 36); for ethylene on graphite these values are 110 (Ref. 32) and 114.2 K (Ref. 37). These differences appear to be larger than what one would

TABLE II. Melting transition of methane on graphite. n is the low-temperature coverage without desorption correction, n_e is the effective coverage at T_p after desorption correction. Due to the shape of the melting boundary, FWHM, peak height, and ΔH are difficult to determine near $n=0.78$. The uncertainty in n_e, due to desorption, ranges from 0.005 for $n_e \leq 0.825$ to 0.015 for $n_e \simeq 1.00$.

	Coverage (n)	Coverage (n_e)	T_p (K)	FWHM (K)	Height (k_B)	ΔH (k_BK)
CH_4	0.076	0.076	56.06	0.5	10	10
	0.145	0.145	56.37	0.2	55	20
	0.184	0.184	56.56	0.15	65	34
	0.204	0.204	56.32	0.15	90	38
	0.207	0.207	56.57	0.15	90	40
	0.251	0.251	56.34	0.15	90	38
	0.297	0.297	56.58	0.15	100	42
	0.395	0.395	56.57	0.15	95	41
	0.467	0.467	56.58	0.15	90	38
	0.525	0.525	56.59	0.15	95	44
	0.536	0.536	56.60	0.15	85	48
	0.588	0.588	56.36	0.15	60	38
	0.627	0.627	56.59	0.15	50	34
	0.669	0.669	56.60	0.2	65	35
	0.704	0.704	56.34	0.6	35	30
	0.052	0.752	57.17	>3	~5	
	0.775	0.775	59.82	>3	~5	
	0.805	0.805	75.60	>5	~2	
	0.811	0.811	84.00	4	11	57
	0.825	0.82	85.00	3	18	84
	0.853	0.83	87.50	1.5	23	67
	0.880	0.865	86.66	1.5	25	55
	0.990	0.915	90.96	1.5	28	64
	1.015	0.93	91.60	1.0	40	83
	1.031	0.935	92.00	1.0	40	60
	1.080	0.94	93.70	0.8	60	91
	1.180	0.965	95.00	0.7	60	87
	1.225	0.99	95.37	0.5	70	80
	1.301	1.00	96.11	0.5	55	73
CD_4	0.211	0.211	56.21	0.15	82	40
	0.381	0.381	56.09	0.15	85	40
	0.552	0.552	56.00	0.15	85	40

expect from different temperature scales from different laboratories. We believe the value based on the heat capacity studies are more reliable. This is the case because the liquid-vapor coexistence boundary is almost perpendicular to the temperature axis over a wide coverage range near n_c and heat-capacity scans, made at constant coverage as a function of temperature intercept the boundary perpendicularly. Vapor pressure isotherms rely upon "vertical risers" of the coverage versus pressure plot to determine region of two phase coexistence. This is not a sensitive method for T near T_c. Since the compressibility of the adsorbed system, or the derivative of the isotherm, diverges near $T=T_c$, i.e., $\partial n/\partial p \sim (T_c - T)^{-\gamma}$, the isotherms taken slightly above T_c may appear to have a vertical riser. A number of isotherm experiments determine T_c by extrapolating the compressibility versus temperature plot from isotherms taken at $T > T_c$. This procedure always overestimates T_c since the critical exponent γ characterizing the compressibility of a two-dimensional liquid-vapor transition is equal to 1.75 rather than 1.[38] The characteristics of the liquid-vapor transition of methane on graphite as a function of surface coverage are shown in Table III.

In addition to the scans of CH_4 on graphite, Fig. 5 also shows a scan of CD_4 on graphite near the liquid-vapor transition at $n=0.381$. At this coverage, the transition temperature is essentially the two-dimensional critical temperature. It can be seen in Fig. 5 that the critical temperature of CD_4 on graphite is 0.3 K lower than that of CH_4. A similar isotopic effect is observed in the three-dimensional critical temperatures. For CH_4, the critical temperature is 190.64 K and for CD_4, it is 189.2 K.[39] In addition to the effect of mass difference (which suggest CD_4 should have a higher critical temperature), the critical temperature of a system also increases with the depth of the intermolecular potential well. The well depth is roughly proportional to the square of the molecular polarizability, and the polarizability of the deuterated molecule

TABLE III. Liquid-vapor transition of submonolayer methane on graphite.

	Coverage (n)	T_p (K)	FWHM (K)	Height (k_B)	ΔH (k_BK)
CH_4	0.145	62.65	4	6	20
	0.184	66.15	6	3	10
	0.204	66.70	4	7	26
	0.207	67.82	7	6	28
	0.256	68.51	5	8	35
	0.279	68.69	4	8	34
	0.308	68.80	6	7	30
	0.341	68.71	5	7	33
	0.346	68.69	3	6	26
	0.368	68.77	5	6	21
	0.394	68.65	5	6	20
	0.395	68.61	6	7	21
	0.424	68.70	6	5	14
	0.453	68.64	5	4	8
	0.490	68.73	5	5	17
	0.525	68.63	7	3	7
	0.559	68.57	7	4	8
	0.574	68.42	8	2	7
	0.588	68.10	5	3	6
	0.591	67.15	6	2	5
	0.602	66.80	7	2	6
	0.627	66.60	7	3	3
	0.641	64.81	5	2	5
CD_4	0.211	68.40	5	8	30
	0.381	68.40	7	6	25
	0.552	67.50	6	3	6

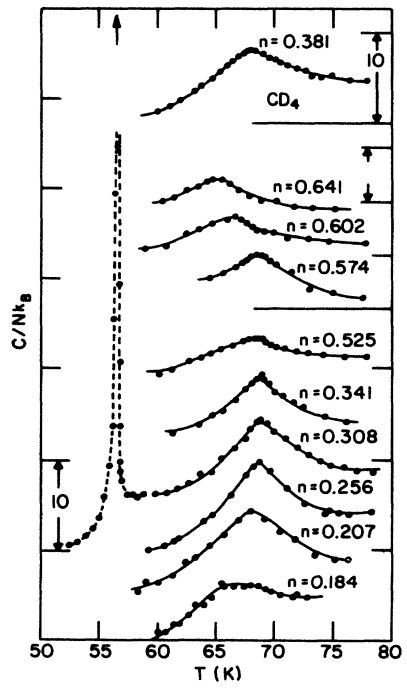

FIG. 5. Heat-capacity scans of submonolayer methane on graphite in the liquid-vapor transition region. The top scan of $n=0.381$ is from CD_4 and the others are from CH_4. The sharp peak near 57 K is related to melting transition, for clarity, this is shown for only one coverage.

is smaller than that of the nondeuterated molecule.[39] In the case of methane, the potential term appears to win out. A similar isotopic effect also is seen in the two-dimensional critical temperature of ethylene on graphite, for C_2H_4 the critical temperature is 110 K and for C_2D_4 it is 107.7 K.[32]

The isotopic effect seen for the critical temperature is similar for the two-dimensional and three-dimensional melting triple points of methane discussed in the section of submonolayer melting. The explanation given above for the critical temperature is probably also valid in the melting transition. The isotopic effect we found in the CIT of methane on graphite is in the reverse direction; at submonolayer coverages, CIT occurs at a lower temperature for CH_4 than for CD_4. This appears to indicate that in this transition where the substrate periodicity plays a central role, the effect due to the mass difference, rather than the intermolecular potential between the adsorbate molecules, is more important.

VII. PHASE TRANSITIONS IN THE MONOLAYER COMPLETION REGION

Figure 6 shows heat-capacity traces of four different coverages between $n=0.853$ to 1.301 at temperatures between 60 and 100 K. In this coverage and temperature region, desorption of the adsorbate molecules into the sample cell volume surrounding the calorimeter is important.

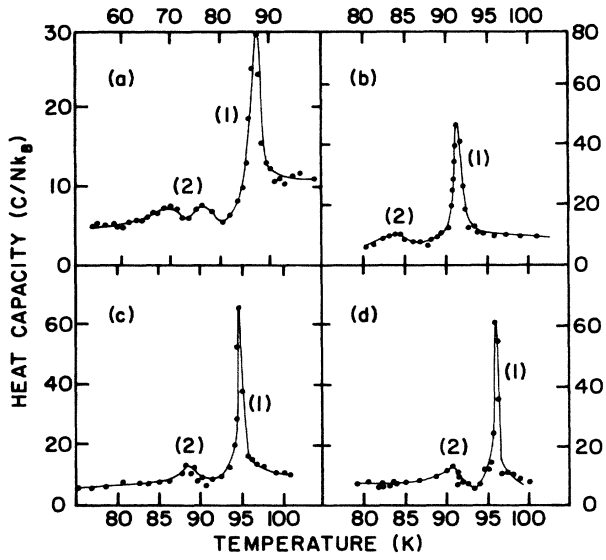

FIG. 6. Heat-capacity scans of high-coverage CH_4 on graphite for (a) $n=0.853$, (b) $n=1.031$, (c) $n=1.180$, and (d) $n=1.301$. The sharp peaks labeled by (1) represent melting transition from expanded solid to fluid, and the broad peaks labeled by (2) represent the DS-CS-ES transition. For $n=0.853$, there are two broad peaks suggesting that in this coverage the transitions proceed from DS to CS and from CS to ES. In other coverages these two peaks are merged into one. The effective coverages at the melting temperatures are (a) $n_e=0.83$, (b) $n_e=0.935$, (c) $n_e=0.965$, and (d) $n_e=1.00$. The effective coverages at the DS-CS-ES transition temperatures are (a) $n_e=0.85$, (b) $n_e=0.98$, (c) $n_e=1.00$, and (d) $n_e=1.025$.

In the discussion and the figures below, the effective surface coverage n_e after desorption correction at the transition temperatures as well as the low temperature coverage, n, with no desorption correction, are given to label these traces. Two heat-capacity peaks are seen for the three scans at higher coverages and three peaks are seen for the $n=0.853$ scan. The highest temperature peak is narrow and sharp; at $n=1.301$, the height and half width (FWHM) are $55k_B$ per molecule and 0.5 K, respectively. We interpret this peak to be related to the melting transition. The sharpening of this peak with coverage (from $n=0.853$ to 1.301) is related to the fact that the experimental path is becoming more perpendicular to the melting phase boundary. The identification of this signature as melting is in general agreement with neutron and NMR results.[1,2,4]

The peak or peaks at lower temperature for these traces are related to transitions in the adsorbed solid. Careful vapor pressure isotherm studies in the near monolayer completion region were performed at 70, 78, 85, 89.6, 93.4, and 97 K to complement the heat-capacity measurements. Figure 7 shows the isotherms taken at 85 and 93.4 K. The 85-K isotherm exhibits two clear anomalies, the one at the lower coverage ($n_e \sim 0.82$) corresponds to the melting and the one at higher coverage ($n_e \sim 0.93$), a transition in the solid overlayer. Whereas the melting transition appears prominently in the 93.4-K isotherm near $n_e \sim 0.93$, the transition in the solid phase in higher coverage cannot be easily identified. In order to examine the isotherm result more careful, the compressibility, or the derivative of the isotherm, i.e., $(1/n)(\partial n/\partial p)$ as a function of coverage is calculated via a computer program. Figure 8 shows the compressibility as a function of effective coverage at four temperatures. These isothermal compressibility plots show two anomalies and the locations of these anomalies, $n(T)$, are consistent with the locations of the peaks in the heat-capacity scans. The lower coverage compressibility anomaly, as stated above, can be naturally identified to be that due to melting. Whereas the size of the higher coverage compressibility anomaly is of the same order as that of melting for the $T=78$- and 85-K isotherms, they are about 2 orders of magnitude smaller for the 89.6- and 93.4-K isotherms.

Based on the information from the heat-capacity and vapor-pressure isotherm scans, a tentative phase diagram in this coverage-temperature region is shown in Fig. 9. The coverage shown reflects desorption effect. Along a path of constant coverage near $n=0.90$, the phase diagram of Fig. 9 proposes consecutively with increasing temperature a region of incommensurate dense solid (DS), a sliver of commensurate $(\sqrt{3}\times\sqrt{3})$ solid (CS), a region of incommensurate expanded solid (ES), a region of coexisting expanded solid and liquid, and finally a liquid (L) region. The presence as well as the locations of the DS and ES regions are consistent with the neutron results.[1] The neutron scattering study found a DS phase in the region of low temperature and at coverages above the commensurate value, and that melting always proceeds from

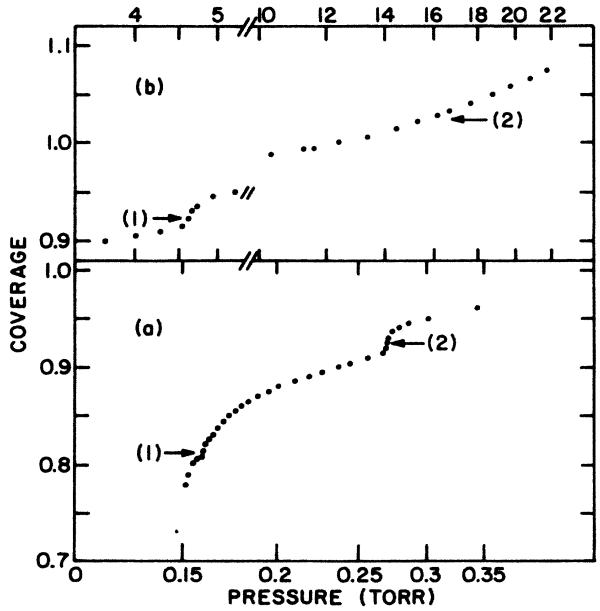

FIG. 7. Adsorption isotherms of CH_4 on graphite at (a) $T=85.0$ K and (b) $T=93.4$ K. Coverage $n=1$ corresponds to the completion of first monolayer solid at 78 K. Regions labeled (1) and (2) represent, respectively, melting transition and ES-CS-DS transitions. The location of the anomalies are in reasonable agreement with locations of heat-capacity peaks in Fig. 6.

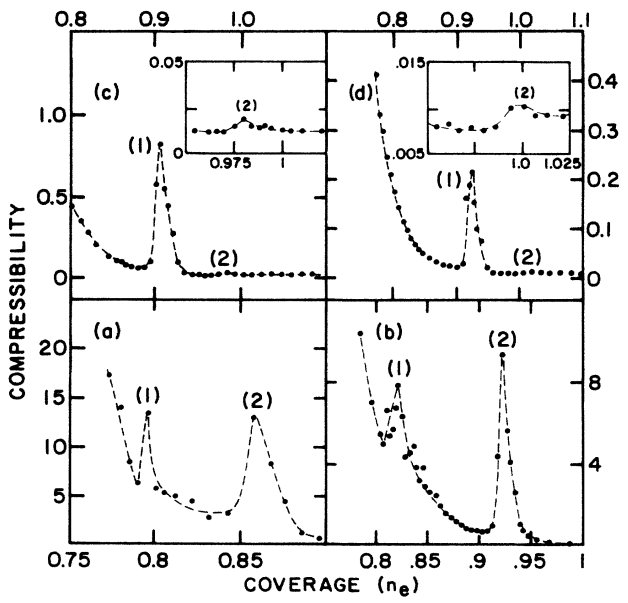

FIG. 8. Compressibility versus coverage at (a) $T=78.0$ K, (b) $=85.0$ K, (c) 89.6 K, and (d) $=93.4$ K of CH_4 on graphite. Peaks labeled (1) and (2) come from steps or kinks (1) and (2) in Fig. 7 by differentiating pressure against coverage, respectively. Peaks (1) and (2) correspond to melting and ES-CS-DS transitions. Note the different compressibility scales at different temperatures. The anomaly related to the ES-DS transition for 89.6 and 93.4 K are shown in greatly expanded compressibility scales in the insets.

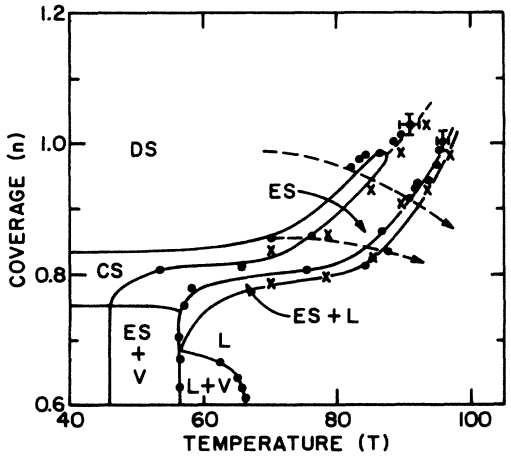

FIG. 9. Phase diagram of methane on graphite in the high-temperature and high-surface-coverage region. Solid lines represent phase boundaries. Dashed arrows correspond to the real experimental path after desorption correction. Closed circles are locations of observed heat-capacity peaks and crosses are location of steps or kinks of adsorption isotherm data. Due to desorption, the uncertainity in the effective coverage ranges from the size of data point (0.005) for $n_e \simeq 0.80$ to 0.015 for $n_e \simeq 1.0$. Uncertainty in T_p for the DS-CS-ES transition is about 2 K, and that of melting 0.5 K (see Tables II and IV).

the ES phase. Since the neutron, NMR, and our heat-capacity results indicate a first-order transition of melting, the ES + L region is consistent with this interpretation. Along a coverage near $n_e = 1$, however, the sliver of the CS phase that exists between the DS and the ES phases is either exceedingly narrow or it is not present. (It should be pointed out that transition between the DS, CS, and ES phases at a constant coverage and the existence of an ES near $n_e = 1$ indicate that the second layer is acting as a reservoir for the monolayer.) Our interpretation of a narrow sliver of the CS phase that extends from low temperature and terminates near $n_e = 1.0$ and $T = 88$ K, is based on the abrupt change in the compressibility peak between 85 and 89.6 K. This interpretation suggests that for $n_e < 1$ and $T \leq 88$ K, the change from DS to ES proceeds through the locking-in to a $(\sqrt{3} \times \sqrt{3})$ CS phase that is favored by the graphite substrate. Due to the narrow width of the CS phase and limited resolution of our data, it is not possible for us to determine the nature of the DS to CS to ES transition. It is possible that both the DS to CS and CS to ES transitions are similar to the CIT of Kr (Ref. 40) and N_2 (Ref. 41) on graphite at high coverage and high temperature and the transition includes a fluid-like chaotic phase sandwiched between the commensurate and incommensurate solid (Ref. 42). The heat-capacity scan at $n = 0.853$ shows two peaks in this region; it is reasonable to identify these two peaks, with increasing temperature, as entering the CS phase from the DS region and leaving the CS phase. The characteristics of the heat-capacity peak corresponding to the transition from the DS to ES are presented in Table IV.

As stated above, the distinctly different compressibility signature below and above 88 K let us to suggest that the CS region terminates near $n_e = 1$ and $T = 88$ K. One reasonable interpretation for the compressibility result is that due to the increase in thermal energy and chemical potential of the overlayer for $n_e \geq 1$ and $T \geq 88$ K, the locking-in to a CS phase between the DS and ES phase by the substrate is no longer favorable and transition between DS and ES phases is a continuous process. It should be noted that heat-capacity scans do not show a corresponding qualitative change in the same coverage and temperature region. Even in a continuous DS-ES transition, the substrate is likely to have the residual effect of accelerating the change in the density of the overlayer when the overlayer density matches the commensurate value. A rapid or accelerated change in density can give rise to the observed heat-capacity anomalies seen for $T > 88$ K and $n_e > 1$.

In the neutron study,[1] no evidence of a phase transition was found when scans were made from the DS to ES region. Instead, a smooth change in the lattice constant was found. In the neutron phase diagram, the CS phase was proposed to terminate near $T = 70$ K and $n = 0.87$, without extending as a thin sliver to higher (i.e., 88 K) temperatures. A reasonable explanation for the difference

TABLE IV. Transition from compressed to expanded solids. The uncertainties in n_e, due to desorption corrections, range from 0.005 for n_e near 0.8 to 0.015 for n_e near 1.0.

Coverage (n)	Coverage (n_e)	T_p (K)	FWHM (K)	Height (k_B)	ΔH (k_BK)
0.811	0.811	65.6	4	2	5
0.853	0.85	70.0[a]	5	3	15
		76.3[a]	5	3	10
0.990	0.96	82.0	3	3	12
1.015	0.975	83.6	3	4	15
1.021	0.98	84.3	3	3	12
1.080	0.98	86.6	3	6	20
1.180	1.00	88.4	3	6	16
1.225	1.01	89.4	3	7	20
1.301	1.025	90.9	3	7	27

[a]Two peaks were seen at $n = 0853$.

between our phase diagram and the neutron one is related to substrate finite size and heterogeneity effects. In the neutron scattering experiment, Grafoil, another exfoliate graphite substrate, rather than Graphite Foam is used as the substrate. Substrate heterogeneity effect in Grafoil, due to the much smaller single-crystal domain size at approximately (100 Å)^2 is far more serious than in Graphite Foam with domain size of about (1000 Å)^2.[14] Graphite Foam is used in our experiment. Whereas the locking-in of the CS phase is still observable on Graphite Foam, it is smeared out on Grafoil. This high-coverage—high-temperature region of CH_4 on graphite was also examined in recent vapor-pressure isotherm and heat of adsorption study.[10] This study appeared to have missed quite a bit of the details reported here.

Because of serious desorption of the adsorbate molecules, it is not possible in our experimental setup to maintain an effective coverage of $n_e > 1.0$ on the graphite surface for $T > 95$ K. We are therefore not able to follow the melting transition to higher coverage. It is reasonable to expect that at higher surface coverage, the melting temperature will decrease with coverage. Recent measurements focusing on the melting of multilayer methane on graphite suggest that the melting temperature for $n > 1$ approaches smoothly the bulk triple temperature with increasing coverage.[43]

In conclusion, the monolayer methane on graphite system has shown to be a particularly interesting system in physical adsorption. The liquid-vapor transition, being at a convenient temperature region, allows us to show quantitatively that the two-dimensional liquid-vapor critical point belongs to the two-dimensional Ising universality class. The nature of the commensurate-incommensurate transitions of the solid overlayer is dependent on whether there is a coexisting 2D vapor phase. We have also found evidence of a novel locking-in phenomenon where a thin sliver of the CS phase intrudes between two incommensurate phases up to a high temperature. The existence and the termination of this thin sliver of the CS phase clearly demonstrate the delicate balance of substrate-adsorbate and adsorbate-adsorbate interaction at a finite temperature.

Our measurements on CD_4 in addition to CH_4 provide reliable information on the isotopic effect in two-dimensional phase transitions. For liquid-vapor and melting transitions, the transition temperature of the CD_4 system is lower than that of CH_4. In the CIT transition, the reverse is found.

ACKNOWLEDGMENTS

We acknowledge useful discussions with W. A. Steele, S. K. Sinha, M. R. Giri, and J. Z. Larese. This work is supported by the National Science Foundation through Grant Nos. DMR-8419261 and DMR-8206109 (low-temperature physics).

*Present address: Department of Physics, Pusan National University, Pusan, Korea.

[1]P. Vora, S. K. Sinha, and R. K. Crawford, Phys. Rev. Lett. **43**, 704 (1979). P. Vora, Ph.D. thesis, University of Illinois, 1980.

[2]P. Dutta, S. K. Sinha, P. Vora, M. Nielsen, L. Passell, and M. Bretz, in *Ordering in Two Dimensions*, edited by S. K. Sinha (North-Holland, New York, 1980), p. 169; A. Glachant, J. P. Coulomb, M. Bienfait, and J. G. Dash, J. Phys. Lett. **40**, L543 (1979); I. Marlow, R. K. Thomas, T. D. Trewern, and J. W. White, J. Phys. Colloq. **38**, C4-19 (1977).

[3]R. Beaume, J. Suzanne, J. P. Coulomb, and A. Glachant, Surf. Sci. **137**, L1117 (1984).

[4]J. H. Quatemann and M. Bretz, Phys. Rev. Lett. **49**, 267 (1982); Phys. Rev. B **29**, 1159 (1984).

[5]J. Z. Larese and R. J. Rollefson, Phys. Rev. B **31**, 3048 (1985).

[6]R. Marx and E. F. Wassermann, Surf. Sci. **117**, 267 (1982).

[7]O. Ferreira, C. C. Colucci, E. Lerner, and O. E. Vilches, Surf. Sci. **146**, 309 (1984).

[8]J. P. Coulomb, M. Bienfait, and P. Thorel, J. Phys. (Paris) **42**, 293 (1981); Phys. Rev. Lett. **42**, 733 (1979).

[9]A. Thomy and X. Duval, J. Chem. Phys. **67**, 286 (1970); **67**, 1101 (1970).

[10]A. Inaba, Y. Koga, and J. A. Morrison, J. Chem. Soc. Faraday Trans. 2 (to be published).

[11]J. M. Gay, A. Dutheil, J. Krim, and J. Suzanne (unpublished).

[12]H. K. Kim and M. H. W. Chan, Phys. Rev. Lett. **53**, 170 (1984).

[13]H. K. Kim, Q. M. Zhang, and M. H. W. Chan, J. Chem. Soc. Faraday Trans. 2 (to be published).

[14]R. J. Birgeneau, P. A. Heiney, and J. P. Pelz, Physica (Utrecht) **109&110**, 1785 (1982).

[15]K. D. Miner, M. H. W. Chan, and A. D. Migone, Phys. Rev. Lett. **51**, 1465 (1983).

[16]M. H. W. Chan, A. D. Migone, K. D. Miner, and Z. R. Li, Phys. Rev. B **30**, 2681 (1984); P. F. Sullivan and G. Seidel, Phys. Rev. **173**, 679 (1968).

[17]*Thermophysical Properties of Matter*, edited by Y. S. Touloukian (IFI/Plenum, New York, 1970); C. Uher, Cryogenics **20**, 445 (1980).

[18]Q. M. Zhang, H. K. Kim, and M. H. W. Chan, Phys. Rev. B **32**, 1820 (1985); A. D. Migone, H. K. Kim, M. H. W. Chan, J. Talbot, D. J. Tildesley, and W. A. Steele, Phys. Rev. Lett. **51**, 192 (1983); R. D. Diehl, M. F. Toney, and S. C. Fain, Jr., *ibid.* **48**, 177 (1982).

[19]H. You and S. C. Fain, Jr., Surf. Sci. **151**, 361 (1985); K. Morishige, C. Mowforth, and R. K. Thomas, *ibid.* **151**, 289 (1985); Y. P. Feng and M. H. W. Chan (unpublished).

[20]P. K. Kubik, W. N. Hardy, and H. Glatti, Can. J. Phys. **63**, 605 (1985).

[21]A. J. Berlinsky and A. B. Harris, Phys. Rev. Lett. **40**, 1579 (1978); Can. J. Phys. **57**, 1852 (1979); C. R. Fuselier, N. S. Gillis, and J. C. Raich, Solid State Commun. **25**, 747 (1978).

[22]S. F. O'Shea and M. L. Klein, J. Chem. Phys. **71**, 2399 (1979); K. Maki and S. Nose, *ibid.* **71**, (1979); E. S. Severin and D. J. Tildesley (unpublished).

[23]J. Bruno and M. R. Giri, Phys. Rev. B **25**, 6711 (1982).

[24]M. W. Newberry, T. Raymont, M. V. Smalley, R. K. Thomas, and J. W. White, Chem. Phys. Lett. **59**, 461 (1978); M. V. Smalley, A. Huller, R. K. Thomas, and J. W. White, Mol. Phys. **44**, 533 (1981).

[25]S. V. Hering and O. E. Vilches, J. Low Temp. Phys. **25**, 793 (1976).

[26]J. M. Phillips. Phys. Rev. B **29**, 4821 (1984).

[27]J. A. Litzinger and G. A. Stewart, in *Ordering in Two Dimensions,* edited by S. K. Sinha (North-Holland, New York, 1980), p. 267.

[28]G. B. Huff and J. G. Dash, J. Low Temp. Phys. **24**, 155 (1976).

[29]J. Stoltenberg and O. E. Vilches, Phys. Rev. B **22**, 2920 (1980).

[30]Q. M. Zhang, H. K. Kim, and M. H. W. Chan, Phys. Rev. B **33**, 5149 (1986).

[31]K. Clusius and L. Popp, Z. Phys. Chem. (Leipzig) B **46**, 63 (1940); A. Kruis, L. Popp, and K. Clusius, Z. Elektrochem. **43**, 664 (1937).

[32]H. K. Kim, Q. M. Zhang, and M. H. W. Chan, Phys. Rev. Lett. **56**, 1579 (1986); H. K. Kim, Q. M. Zhang, Y. P. Feng, and M. H. W. Chan (unpublished).

[33]L. Onsager, Phys. Rev. **65**, 117 (1944); Nuovo Cimento **6**, 261 (1949); C. N. Yang, Phys. Rev. **85**, 808 (1952).

[34]A. D. Migone, Z. R. Li, and M. H. W. Chan, Phys. Rev. Lett. **53**, 810 (1984).

[35]F. Millot, J. Phys. (Paris), Lett. **40**, L9 (1979); Y. Lahrer and B. Gilqun, Phys. Rev. A **20**, 1599 (1979).

[36]P. Dolle, M. Matecki, and A. Thomy, Surf. Sci. **91**, 271 (1980).

[37]J. Menaucourt, A. Thomy, and X. Duval, J. Phys. (Paris) Colloq. **38**, C4-195 (1977).

[38]See comments by M. E. Fisher and M. H. W. Chan, J. Chem. Soc. Faraday Trans. 2 (to be published).

[39]A. F. Grigor and W. A. Steele, J. Chem. Phys. **48**, 1032 (1968); **48**, 1038 (1968).

[40]P. W. Stephens, P. A. Heiney, R. J. Birgeneau, P. M. Horn, D. E. Moncton, and G. S. Brown, Phys. Rev. B **29**, 3512 (1984); E. E. Specht, M. Sutton, R. J. Birgeneau, D. E. Moncton, and P. M. Horn, *ibid.* **30**, 1589 (1984); K. L. D'Amico, D. E. Moncton, E. D. Specht, R. J. Birgeneau, S. E. Nagler, and P. M. Horn, Phys. Rev. Lett. **33**, 2250 (1984).

[41]M. Bjurstrom and M. H. W. Chan (unpublished).

[42]S. N. Coppersmith, D. S. Fisher, B. I. Halperin, P. A. Lee, and W. F. Brickman, Phys. Rev. Lett. **46**, 549 (1982); Phys. Rev. B **25**, 349 (1982); M. Kadar and A. N. Berker, Phys. Rev. Lett. **48**, 1552 (1982); R. G. Calflisch, A. N. Berker, and M. Kardar, Phys. Rev. B **31**, 4527 (1985); D. A. Huse and M. E. Fisher, Phys. Rev. Lett. **49**, 793 (1982); Phys. Rev. B **29**, 229 (1984).

[43]J. J. Hamilton and D. L. Goodstein, Phys. Rev. B **28**, 3838 (1983); D. L. Goodstein, J. J. Hamilton, M. J. Lysek, and G. Vidali, Surf. Sci. **148**, 187 (1984).